

Contractor renormalization group theory of $SU(N)$ chains and ladders

Peng Li and Shun-Qing Shen

Department of Physics, The University of Hong Kong, Pokfulam Road, Hong Kong, China

(Received 8 December 2004; revised manuscript received 7 March 2005; published 1 June 2005)

The contractor renormalization group (CORE) method is applied to the $SU(N)$ chain and ladders in this paper. In our designed schemes, we show that these two classes of systems can return to their original form of Hamiltonian after CORE transformation. Successive iteration of the transformation leads to a fixed point so that the ground state energy and the energy gap to the ground state can be deduced. The result of $SU(N)$ chain is compared with the one by Bethe ansatz method. The transformation on spin-1/2 ladders gives a finite gap in the excited energy spectra to the ground state in an intuitive way. The application to $SU(3)$ ladders is also discussed.

DOI: 10.1103/PhysRevB.71.212401

PACS number(s): 75.10.Pq, 64.60.Ak, 05.50.+q

The contractor renormalization (CORE) group method combines the contraction and cluster expansion techniques with the real space renormalization group approach to solve the electron and spin lattice problems.¹ It was first applied to spin-1/2 Heisenberg chain and (1+1)-dimensional Ising model, and later to the frustrated antiferromagnets and the Haldane conjecture. The results are satisfactory and encouraging.^{1,2} Since then the method has been applied to investigate low energy physics in many strongly correlated systems.³⁻⁸ In this paper, we are concerned with a class of models showing that CORE is at its *critical point*, which means that the symmetry of the system is restored or the same form of Hamiltonian is reconstructed after the CORE transformation, just like the spin-1/2 Heisenberg chain.¹ Undoubtedly, this method is not limited to such a kind of systems. Though in many systems the original Hamiltonian cannot be recovered, the lower energy physics are retained and studied successively after the truncation and transformation.

We consider the $SU(N)$ chain and ladders in this work. We show that the same form of the Hamiltonian is recovered after dividing adequately the lattice into blocks and defining a truncation scheme, so that the CORE algorithm can be done recursively. The range-2 result for $SU(N)$ chain is compared with the Bethe ansatz solution by Sutherland.⁹ The comparison suggests that the CORE method can give good result especially for large N and relatively larger blocks. We also present the results of the real-space renormalization group (RG) theory, which usually agrees qualitatively with the one by range-2 CORE calculation.² In many cases the latter can be regarded as a refined method on the former. The spin-1/2 ladders have attracted a lot of attention since the discovery of a finite spin gap in the two-leg ladders.^{10,11} Another CORE scheme based on plaquette dividing of the ladder had been applied to this system.^{7,12} Here we shall use a different scheme which shows a $S=1$ magnon gap in an intuitive way. Results up to range-3 are presented.

It was shown by Morningstar and Weinstein that the CORE scheme of three-site block partition and two-state truncation on $SU(2)$ chain recover the original form of Hamiltonian. Then the resulting effective Hamiltonian can be solved iteratively and a quite satisfactory result can be obtained.¹ The recovery of the form of the Hamiltonian owes

highly to the $SU(2)$ symmetry and an adequate designed CORE scheme. As a generalization, we found that their CORE scheme on $SU(2)$ chain is a specimen picked out from a general CORE scheme on the $SU(N)$ chain. Though the $SU(N)$ chain had been exactly solved by Bethe ansatz method long time ago,⁹ it is still instructive to see how CORE works in the system.

Let us start with a one-dimensional $SU(N)$ chain in terms of the exchange operator, $H=J\sum_j P_{j,j+1}$. Here we limit our discussion to the antiferromagnetic case by setting $J=1>0$. For a $SU(N)$ system each site j has N quantum states $|j, \alpha\rangle$ with $(\alpha=1, 2, \dots, N)$. The exchange operator $P_{j,j+1}$ swaps two states on sites j and $j+1$, i.e., $P_{j,j+1}|j, \alpha; j+1, \beta\rangle = |j, \beta; j+1, \alpha\rangle$. Usually $P_{j,j+1}$ can be expressed in terms of the $SU(N)$ generators as $P_{j,j+1} = \sum_{\alpha\beta} J_{\beta}^{\alpha}(j) J_{\alpha}^{\beta}(j+1)$, where the operators $J_{\beta}^{\alpha}(j)$ satisfy the $SU(N)$ algebra $[J_{\beta}^{\alpha}(j), J_{\nu}^{\mu}(j')] = \delta_{jj'} [\delta_{\nu}^{\alpha} J_{\beta}^{\mu}(j) - \delta_{\beta}^{\mu} J_{\nu}^{\alpha}(j)]$. Alternatively, $P_{j,j+1}$ can also be expressed by spin operators.^{13,14} Many spin systems as well as spin-orbital systems concerning $SU(N)$ symmetry have been studied extensively.¹⁵⁻¹⁹

In the CORE scheme, the first step is to divide the original chain into a chain of blocks and retain adequate number of energy levels in each block. We found two obvious schemes to be readily applied to this system: one is $(N-1)$ -site block partition with N -state truncation (scheme A), and the other is $(N+1)$ -site block partition with N -state truncation (scheme B). The treatment on $SU(2)$ case in Ref. 1 obviously falls into scheme B with $P_{j,j+1} = 2\mathbf{S}_j \cdot \mathbf{S}_{j+1} + 1/2$ when $N=2$. We will see the scheme B gives better results than scheme A. The existence of the two schemes can be understood from the single column Young tableaux with $(N-1)$ or $(N+1)$ boxes. In fact the $SU(N)$ model on both $(N-1)$ -site block and $(N+1)$ -site block have one unique N -dimensional ground state space. We denote the truncated space for a single block by $\Phi_j = \{|\phi_{j,1}\rangle, |\phi_{j,2}\rangle, \dots, |\phi_{j,N}\rangle\}$. Then in the range-2 CORE calculation, we should retain appropriate N^2 low levels from the exact diagonalization of two blocks. All the retained low levels should have nonzero projection to the product space $\Phi_j \otimes \Phi_{j+1}$, so the eligible levels are not always the lowest ones. Fortunately this job is easy to be done due to the $SU(N)$ symmetry. The range-2 CORE calculation leads to the effective Hamiltonian

TABLE I. The coefficients C_{\mp} and K_{\mp} in Eq. (1).

Scheme A		RG		Range-2 CORE	
N	C_{-}	K_{-}	C_{-}	K_{-}	
3	$\frac{3}{4}$	$\frac{1}{4}$	1.0731	0.3411	
4	$\frac{16}{9}$	$\frac{1}{9}$	2.2485	0.1787	
5	$\frac{45}{16}$	$\frac{1}{16}$	3.3762	0.1112	
Scheme B		RG		Range-2 CORE	
N	C_{+}	K_{+}	C_{+}	K_{+}	
2	$\frac{13}{18}$	$\frac{4}{9}$	0.9956	0.4916	
3	2.1693	0.2654	2.5982	0.3084	
4	3.4111	0.1728	3.9432	0.2089	

$$H^{(2)} = \frac{1}{N \mp 1} \sum_j (-C_{\mp} + K_{\mp} \tilde{P}_{j,j+1}), \quad (1)$$

where the sign \mp corresponds to the two schemes A (-) and B (+), $\tilde{P}_{j,j+1}$ is a renormalized exchange operator connecting blocks j and $j+1$ after each block “contracts” to a single site. The coefficients C_{\mp} and K_{\mp} are listed in Table I. It can be confirmed the range-3 Hamiltonian will include another operator $\tilde{P}_{j,j+2}$ and the range-4 Hamiltonian will include more operators like $\tilde{P}_{j,j+3}$, $\tilde{P}_{j,j+1}\tilde{P}_{j+2,j+3}$, $\tilde{P}_{j,j+2}\tilde{P}_{j+1,j+3}$, $\tilde{P}_{j,j+3}\tilde{P}_{j+1,j+2}$. Here we only give the range-2 results since higher range calculation will not change the physics. For scheme A and B, we give the results for $N=3,4,5$ and $2,3,4$, respectively.

Successive application of CORE in Eq. (1) will lead the running coupling approaching a gapless fixed point. And no phase transition is observed. The ground energy is read out as

$$E_0 = -\frac{C_{\mp}}{(N \mp 1) - K_{\mp}}, \quad (2)$$

where the sign \mp corresponds to the two schemes. Figure 1 shows that the result of the range-2 CORE of scheme B agrees quite well with the one by Bethe ansatz method. The numerical error can be reduced by higher range calculation. The range-4 result for $N=2$ by Weinstein shows the error is reduced to -0.0025 .²

In fact the traditional RG gives an effective Hamiltonian having the same form of Eq. (1). It can produce results consistent with CORE though not so good.² The two schemes above are still applicable and the corresponding coefficients can be found in Table I. The advantages of CORE are obvious. In many cases one can design more flexible schemes in CORE while selecting basic blocks and truncating at low levels.³⁻⁸ A more careful analysis shows that RG based on $(N-1)$ -site block partition scheme (scheme A) can give an effective Hamiltonian for general N ,

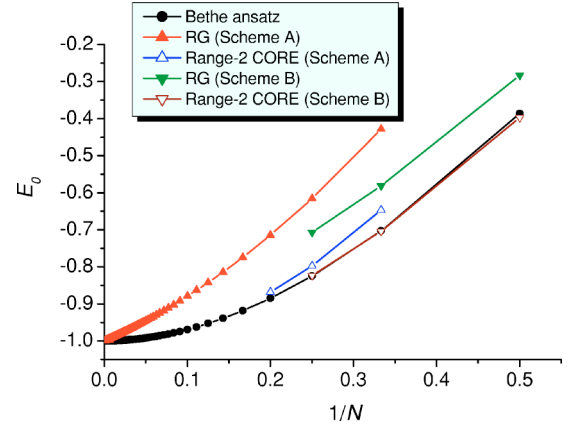


FIG. 1. (Color online) The ground energy of $SU(N)$ chain. Scheme B of CORE gives better results and the numerical errors are about -0.0106 , -0.0006 , 0.0021 for $N=2,3,4$, respectively, compared to the results by Bethe ansatz (see Ref. 9).

$$H^{RG} = \frac{1}{N-1} \sum_j \left[-\frac{N(N-2)^2}{(N-1)^2} + \frac{1}{(N-1)^2} \tilde{P}_{j,j+1} \right], \quad (3)$$

which exhibits a ground energy coinciding with the one by Bethe ansatz method at large N , $E_0 = -N(N-2)/(N^2 - N + 1) \xrightarrow{N \rightarrow \infty} -1$.

The two-leg spin-1/2 ladders aroused a lot of attention when a finite spin gap was observed.¹¹ A simple picture says that the ground state is a product state with the spins on each rung forming a spin singlet. Then the lowest energy excitation is a $S=1$ magnon. Here we show that our scheme of CORE produces exactly the same picture and refined results can be achieved following the CORE algorithm. We start from the Hamiltonian

$$H = \sum_j [(S_j^A \cdot S_{j+1}^A + S_j^B \cdot S_{j+1}^B) + \alpha S_j^A \cdot S_j^B], \quad (4)$$

where the indices A and B refer to the two rails of the ladders, $\alpha = J_{\text{rung}}/J_{\text{rail}}$ is the ratio between the rung and rails couplings, and we have set $J_{\text{rail}} = 1$.

Our first step is to divide the ladder into triads along the rail direction [Fig. 2(a)]. The problem on the rail direction is just the $SU(2)$ chain that had been solved. Detailed calculation shows that the effective interaction between the two blocks along the rung can also recover the Heisenberg interaction. Thus ladders with renormalized couplings can be obtained. The second step is to parse out the effective block-

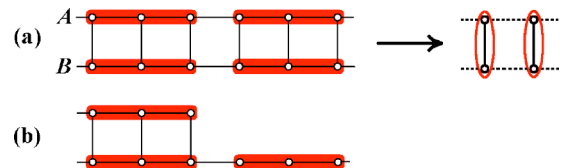


FIG. 2. (Color online) (a) Two-leg ladders. The basic blocks are triads along the rail direction. The fixed point is a chain of decoupled dimers. (b) The unsymmetric configuration of blocks involved in range-3 CORE calculation.

TABLE II. An example of the range-2 CORE iteration procedure at $\alpha=1$.

n	E_0	δ_n	$\Lambda_n(\alpha)$
0	0	1.0	1.0
1	-0.460796	0.491582	0.81919
2	-0.558041	0.241653	0.64499
5	-0.587214	0.028706	0.420144
10	-0.587867	0.000824	0.382715
15	-0.587869	0.000024	0.381603
20	-0.587869	6.7907×10^{-7}	0.381571
21	-0.587869	3.3382×10^{-7}	0.38157
22	-0.587869	1.641×10^{-7}	0.38157

block interactions from all possible configurations of connected blocks. As defined by Morningstar and Weinstein, r connected blocks contain range- r' interactions with $r' = 0, 1, \dots, r$ [$r'=0$ corresponds to the constant term as in Eq. (5)]. To parse out all range interactions the exact diagonalization is employed on the connected blocks. We present range-2 and range-3 results here. It is notable that the range-3 blocks should include a configuration in Fig. 2(b). This unsymmetric configuration may make the iteration procedure more troublesome.

The range-2 CORE result simply regains the original form of Hamiltonian except for a constant term

$$H^{(2)} = \frac{1}{3} \sum_j [-C(\alpha) + \delta(\tilde{\mathbf{S}}_j^A \cdot \tilde{\mathbf{S}}_{j+1}^A + \tilde{\mathbf{S}}_j^B \cdot \tilde{\mathbf{S}}_{j+1}^B) + \Lambda(\alpha)\tilde{\mathbf{S}}_j^A \cdot \tilde{\mathbf{S}}_j^B], \quad (5)$$

where $\delta=0.491582$, $C(\alpha)$ and $\Lambda(\alpha)$ vary with α . The iteration on the range-2 effective Hamiltonian is always applicable because the retained four low levels are always one spin singlet and three spin triplets just like the SU(2) chain case. After n steps of iteration on Eq. (5) we will get running coupling terms as $h_n = \delta_n(\tilde{\mathbf{S}}_j^A \cdot \tilde{\mathbf{S}}_{j+1}^A + \tilde{\mathbf{S}}_j^B \cdot \tilde{\mathbf{S}}_{j+1}^B) + \Lambda_n(\alpha)\tilde{\mathbf{S}}_j^A \cdot \tilde{\mathbf{S}}_j^B$, where the coefficients are determined recursively, $\delta_n = \delta^n$, $\Lambda_n(\alpha) = \delta^{n-1} \Lambda[\Lambda_{n-1}(\alpha)/\delta^{n-1}]$, \dots , $\Lambda_2(\alpha) = \delta \Lambda[\Lambda(\alpha)/\delta]$, $\Lambda_1(\alpha) = \Lambda(\alpha)$, $\Lambda_0(\alpha) = \alpha$. So the rail coupling approaches zero $\delta^n \rightarrow 0$ as $n \rightarrow \infty$, while the rung coupling goes to a fixed value $\Lambda_{n \rightarrow \infty}(\alpha) \neq 0$ for $\alpha > 0$ (we observed that $\Lambda_{n \rightarrow \infty}(\alpha) \rightarrow 0$ only when $\alpha=0$, which is in agreement with the conclusion drawn by DMRG^{10,20} and exact diagonalization).²¹ So the system flows to a fixed point exhibiting dimer covering on each rung of the ladder. The spin gap is read out as $\Delta_s(\alpha) = \Lambda_{n \rightarrow \infty}(\alpha)$. The ground energy E_0 is obtained by cumulating the constant term. Table II gives an example of iterations procedure for $\alpha=1$.

The range-3 CORE result at the first run of iteration contains the next-nearest-neighbor interactions

$$H^{(3)} = \frac{1}{3} \sum_j [-C(\alpha) + \delta(\alpha)(\tilde{\mathbf{S}}_j^A \cdot \tilde{\mathbf{S}}_{j+1}^A + \tilde{\mathbf{S}}_j^B \cdot \tilde{\mathbf{S}}_{j+1}^B) + \Lambda(\alpha)\tilde{\mathbf{S}}_j^A \cdot \tilde{\mathbf{S}}_j^B + \Omega(\alpha)(\tilde{\mathbf{S}}_j^A \cdot \tilde{\mathbf{S}}_{j+1}^B + \tilde{\mathbf{S}}_j^B \cdot \tilde{\mathbf{S}}_{j+1}^A) + \chi(\tilde{\mathbf{S}}_j^A \cdot \tilde{\mathbf{S}}_{j+2}^A + \tilde{\mathbf{S}}_j^B \cdot \tilde{\mathbf{S}}_{j+2}^B)], \quad (6)$$

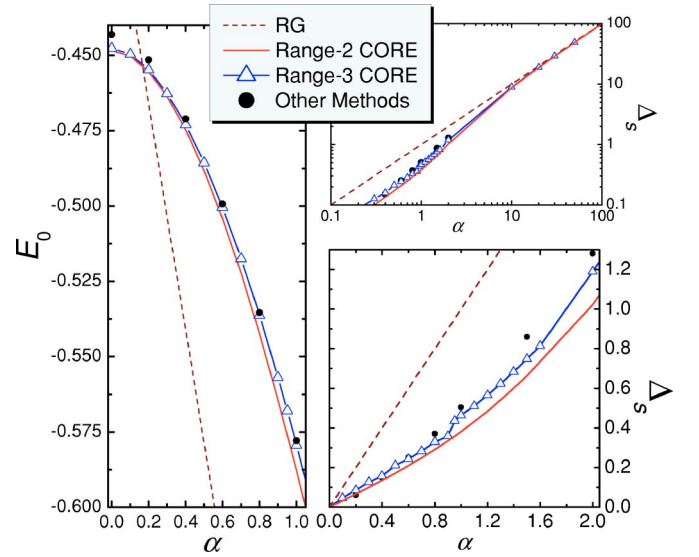


FIG. 3. (Color online) The ground energy and the gap for the spin-1/2 two-leg ladder. The log-log plot shows that CORE and RG give correct gap in strong coupling limit $\alpha \rightarrow \infty$. Data by other methods are adapted from Refs. 11 and 23–25.

where $C(\alpha)$, $\delta(\alpha)$, and $\Lambda(\alpha)$ are different from the ones in Eq. (5), $\gamma=0.033975$. γ will vary with α in the successive iterations, $\gamma_n = \gamma_n(\alpha), \dots, \gamma_1 = \gamma$. After n -step iterations, we found that the only nonvanishing coupling is still the interaction along the rung $\Lambda_{n \rightarrow \infty}(\alpha) \neq 0$, so the physical picture obtained by the range-2 CORE does not change, i.e., the ground energy and the spin gap are produced in the same way.

As we noted above, the unsymmetric configuration of blocks in Fig. 2(b) brings some troubles to the range-3 CORE iteration. Unlike the SU(2) chain, the desired low levels may not always stay at the lowest positions during the iterations. And sometimes it is hard to select out the eligible set of levels from several possible candidates since each of them will lead to a recovered SU(2) symmetry. So different iteration procedures with different results are inevitable. When these situations take place, we resort to the principle: *retaining the iteration procedure that gives the lowest energy*,²² although in our observations the values of the results only have small difference. The range-2 and range-3 CORE results for the ground state energy and the spin gap are illustrated in Fig. 3. For a comparison, data by other methods^{11,23–25} are presented together. The ground energy agrees well with those by other methods in the whole range of interchain coupling α . This means that CORE algorithm can successively capture the low energy physics of the system. The gap has relatively larger deviation at intermediate values of α . Nevertheless the discrepancy can be remedied through higher range CORE calculation. The range-3 gap is a little zigzag. This may be due to the unsymmetric configuration of range-3 blocks in Fig. 2(b). It is noteworthy that RG gives a gap simply as $\Delta_s^{RG} = \alpha$, which captures the correct behaviour of the gap at strong coupling limit $\alpha \rightarrow \infty$.¹¹

We also applied CORE to the two-leg SU(3) ladders, $H = \sum_j [(P_{j,A;j+1,A} + P_{j,B;j+1,B}) + \alpha P_{j,A;j,B}]$. The applicable schemes are presented in Figs. 4(a)–4(c). Notice that all

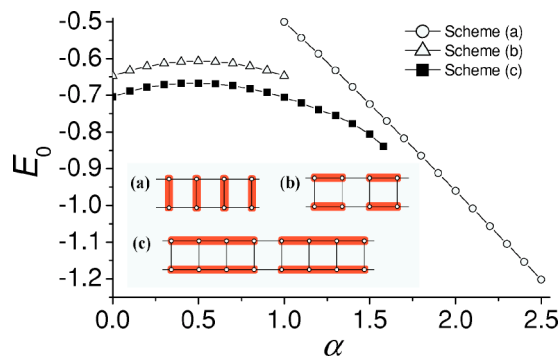


FIG. 4. (Color online) The ground energy of the two-leg SU(3) ladders. The insets (a), (b), and (c) show the schemes used in the calculation.

blocks are equivalent and a three-state truncation is made in each scheme. Scheme (a) should be valid when the rung interaction α is large enough. While for small α , the schemes (a) ($\alpha < 1.0$) and (b) ($\alpha < 1.58$) are appropriate and scheme (b) is better than (a). All three schemes lead to the fixed point with zero gap. We see that scheme (a) will be mapped to a SU(3) chain, which had been solved previously and gives a zero gap. And after the first mapping we applied four-site block partition scheme on the chain in the successive iteration steps to produce the ground energy in Fig. 4. While

scheme (b) and (c) will return to a two-leg SU(3) ladder, $h_n = \delta_n(P_{j,A;j+1,A} + P_{j,B;j+1,B}) + \Lambda_n(\alpha)P_{j,A;j,B}$, but we observed that the running couplings of the rail direction δ_n and the rung direction Λ_n will go to infinitesimals of the same order²⁶ as we push the iteration steps to infinity, $n \rightarrow \infty$, so a gapless phase is also obtained, which agrees with the result of scheme (a). The SU(3) model on a four-leg ladder can be analyzed in similar schemes and a gapless result is also expected. The result is reminiscent of the SU(2) model on a chain and on a three-leg ladder, which are also gapless. But unfortunately the above schemes or their analogs are not applicable for the two-leg SU(4) ladders, which exhibits plaquette singlet-multiplet excitation.^{18,23,27} One may have to resort to other kind of schemes.

In conclusion, we have studied the SU(N) chain and ladders by the CORE schemes. We have shown that the effective Hamiltonian in the appropriate CORE schemes can regain its original form such that it approaches a fixed point by iteration of the CORE schemes. The ground state energy and the lowest excitations can be deduced from the fixed point. The results show that the SU(N) chain and the two-leg SU(3) ladders are gapless, while the two-leg spin-1/2 ladder exhibits gapped phase originated from the rung dimerization.

This work was supported by the Research Grant Council of Hong Kong under the Project No. HKU7038/04P.

¹C. J. Morningstar and M. Weinstein, Phys. Rev. Lett. **73**, 1873 (1994); Phys. Rev. D **54**, 4131 (1996).

²M. Weinstein, Phys. Rev. D **61**, 034505 (2000); Phys. Rev. B **63**, 174421 (2001).

³E. Altman and A. Auerbach, Phys. Rev. B **65**, 104508 (2002).

⁴S. Capponi and D. Poilblanc, Phys. Rev. B **66**, 180503(R) (2002).

⁵E. Berg, E. Altman, and A. Auerbach, Phys. Rev. Lett. **90**, 147204 (2003).

⁶D. Poilblanc, D. J. Scalapino, and S. Capponi, Phys. Rev. Lett. **91**, 137203 (2003).

⁷S. Capponi, A. Lauchli, and M. Mambrini, Phys. Rev. B **70**, 104424 (2004).

⁸R. Budnik and A. Auerbach, Phys. Rev. Lett. **93**, 187205 (2004).

⁹B. Sutherland, Phys. Rev. B **12**, 3795 (1975).

¹⁰E. Dagotto, J. Riera, and D. Scalapino, Phys. Rev. B **45**, R5744 (1992).

¹¹E. Dagotto and T. M. Rice, Science **271**, 618 (1996).

¹²J. Piekarczyk and J. R. Shepard, Phys. Rev. B **57**, 10260 (1998); **60**, 9456 (1999).

¹³E. Schrödinger, Proc. R. Ir. Acad., Sect. A **47**, 39 (1941).

¹⁴P. Li and S. Q. Shen, New J. Phys. **6**, 160 (2004).

¹⁵D. P. Arovas and A. Auerbach, Phys. Rev. B **38**, 316 (1988).

¹⁶N. Read and S. Sachdev, Phys. Rev. B **42**, 4568 (1990).

¹⁷Y. Q. Li, M. Ma, D. N. Shi, and F. C. Zhang, Phys. Rev. Lett. **81**, 3527 (1998).

¹⁸S. Q. Shen, Phys. Rev. B **66**, 214516 (2002); **64**, 132411 (2001).

¹⁹K. Penc, M. Mambrini, P. Fazekas, and F. Mila, Phys. Rev. B **68**, 012408 (2003).

²⁰O. Legeza, G. Fath, and J. Solyom, Phys. Rev. B **55**, 291 (1997).

²¹H. Watanabe, Phys. Rev. B **50**, 13442 (1994).

²²This selection rule should be an important key issue in many iterative methods such as DMRG. See, e.g., S. R. White, Phys. Rev. Lett. **69**, 2863 (1992); Phys. Rev. B **48**, 10345 (1993); O. Legeza and J. Solyom, Phys. Rev. B **70**, 205118 (2004).

²³T. Barnes, E. Dagotto, J. Riera, and E. S. Swanson, Phys. Rev. B **47**, 3196 (1993).

²⁴S. R. White, R. M. Noack, and D. J. Scalapino, Phys. Rev. Lett. **73**, 886 (1994).

²⁵N. Flocke, Phys. Rev. B **56**, 13673 (1997).

²⁶In fact the ratio Λ_n/δ_n will reach at a fixed value 0.3597 for scheme (b) and 1.1176 for scheme (c) as $n \rightarrow \infty$, although $\Lambda_n \rightarrow 0$ and $\delta_n \rightarrow 0$.

²⁷M. van den Bossche, P. Azaria, P. Lecheminant, and F. Mila, Phys. Rev. Lett. **86**, 4124 (2001).